Dust composition and mixing state inferred from airborne composition measurements during ACE-Asia C130 Flight #6

C.H. Song[a,b,*], K. Maxwell-Meier[a], R.J. Weber[a], V. Kapustin[c], A. Clarke[c]

[a]School of the Earth and Atmospheric Sciences, Georgia Institute of Technology, Atlanta, GA, USA
[b]Department of Environmental Science and Engineering, Gwangju Institute of Science and Technology (GIST), Gwangju 500-712, South Korea
[c]Department of Oceanography, University of Hawaii, Honolulu, HI, USA

Abstract

In this study $\sim$3.5 min average bulk aerosol composition data recorded from aircraft during ACE-ASIA C130 Flight #6 are used to investigate the extent of fine particle ($D_{p\ 50} < 1.3\,\mu m$) mixing among various inorganic aerosol particle constituents. Dust-laden air masses that had mixed with urban air pollutants over the Beijing and Tianjin region were subsequently recorded in the marine boundary layer over the Yellow Sea during the ACE-ASIA mission. An analysis of correlations and molar ratios between cations and anions suggest that dust particles are largely composed of $CaCO_3$ (i.e., the dust particles are fresh), and that NH_4^+ and K^+ are likely associated with SO_4^{2-} and NO_3^-. The results point to an external mixture of mineral dust and urban pollutant particles. Aerosol simulations carried out assuming various degrees of internal mixing (by Ca^{2+} mass) between dust and urban particles indicate the observed $2NH_4^+$–SO_4^{2-} association exists only when most of the fine-mode dust particles exist externally to SO_4^{2-}. In this case, the degree of external mixing (by Ca^{2+} mass) is estimated to be larger than 70%.
© 2004 Elsevier Ltd. All rights reserved.

Keywords: Dust mixing state; Ion association; Aerosol thermodynamic modeling; ACE-ASIA campaign

1. Introduction

Atmospheric aerosols are a mixture of various chemical components because they are emitted directly from multiple sources and are secondarily produced by various atmospheric processes. Many researchers have investigated the degree to which atmospheric aerosols are mixed or segregated (e.g., Covert and Heintzenberg, 1984; Zhang et al., 1993; Cooke and Wilson, 1996; Haywood et al., 1997; Kleeman et al., 1997). Two

limiting cases are possible for the degree of aerosol mixing (or segregation): (1) internal mixtures and (2) external mixtures. In the internal aerosol mixture, particles of the same size bins are assumed to have the same chemical composition, whereas, in the external mixture, particles of the same size bin have a different chemical composition. The degree to which aerosol particles mix influences the aerosol chemical composition and determines the aerosol chemical evolution as well as the particle's physical and optical properties.

Measurements of mineral dust, urban pollutants, and sea salt aerosol were made during the Asian Pacific Regional Aerosol Characterization Experiment (ACE-Asia), conducted in the spring of 2001 in East Asia. The

---

*Corresponding author. Department of Environmental Science and Engineering, Gwangju Institute of Science and Technology (GIST), Gwangju 500-712, South Korea.

experiment was a large multi-investigator study involving ground, ship, and airborne measurements, during the time of year when dust storms are most frequent and intense.

In this study, the degree of fine particle mixing is investigated by an indirect method (hereafter, the fine particles are defined as aerosols with diameters nominally smaller than 1.3 μm). Tests are performed on measurements from the ACE-ASIA experiment, and one specific measurement leg from ACE-ASIA C130 Flight #6 is focused on to investigate the aerosol mixing state. The case was encountered in the marine boundary layer (MBL) over the Yellow Sea on April 11, 2001, and contains a complicated mixture of dust, sea-salt, and polluted urban aerosols. Measurements of fine particle ionic composition from the particle into liquid sampler coupled to a dual channel ion-chromatograph (PILS-IC) with an integration period of 3 min 24 s (Weber et al., 2001; Orsini et al., 2003) are used to investigate correlations and molar ratios between various particulate ionic compounds and the results are qualitatively compared to the predictions from a thermodynamic "closed-mode" aerosol model simulation (Jacobson et al., 1996; Meng et al., 1998). This is a unique approach whose benefits and limitations are presented in this paper.

2. Experimental procedures

The PILS-IC measured fine-particle inorganic chemical composition on the C130. In this instrument, sample air is drawn through denuders to remove interfering gases and then rapidly mixed with saturated water vapor. The resulting supersaturated water condenses on the sampled ambient particles that subsequently grow to sizes that are easily captured by inertial impaction onto a small wetted area. With the addition of a small transport flow ($\sim$0.1 ml/min), the resulting liquid flow containing the water-soluble aerosol components is analyzed continuously via anion and cation chromatography. Based on baseline noise from the measurements of ambient air, detection limits are calculated to be in the range of 40–60 ng/m^3 for cations (NH_4^+, Ca^{2+}, Mg^{2+}, K^+, Na^+) and approximately 10–20 ng/m^3 for anions (SO_4^{2-}, NO_3^-, Cl^-). Although it is possible to measure additional ions with the PILS-IC (e.g., carbonate, organic compounds), they were not measured during these airborne experiments since they entail substantially longer integration times for chromatographic separation, thus limiting the sampling rate.

During this experiment, the instrument was operated with a 4-min sampling cycle, with a 3 min 24 s sample integration period (Weber et al., 2001; Orsini et al., 2003). In these experiments the PILS-IC measurements only provided fine-mode aerosol composition, where the

fine-mode is defined here as particles with aerodynamic diameter less than nominally 1.3 μm. At this diameter, the PILS instrument has a 50% collection efficiency. However, the measurement does include larger particles. For example, particles of 2 μm are sampled with an efficiency of approximately $\sim$20%. For more detailed explanations and an experimentally measured efficiency curve, the reader can refer to Maxwell-Meier et al. (2004).

3. Results and discussions

3.1. ACE-ASIA C130 Flight #6

The aerosol mixing state in a chemically complex environment that includes mineral dust particles, polluted urban aerosol particles, and sea-salt particles is analyzed. This type of aerosol mixture was frequently observed during the ACE-Asia experiment. Here the focus is on a portion of the ACE-ASIA C130 Flight #6.

3.1.1. Air trajectories

ACE-ASIA C130 Flight#6 was flown over the Yellow Sea on April 11, 2001. The flight track and 5-day backward trajectories along the flight track are shown in Fig. 1. The aircraft measurements were conducted along a North-South flight track on 124°E longitude between 33° and 37°N latitude. In this analysis we focus on the air masses encountered between 2:15 and 3:11 UTC since they contain both high Ca^{2+} and SO_4^{2-} concentrations, indicating that the measurements are highly impacted by dust and anthropogenic particles. The
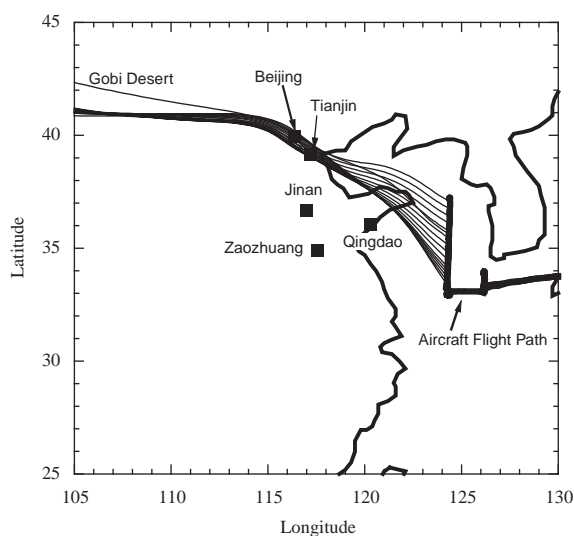

Fig. 1. C130 Flight #6 backward air mass trajectories along the C130 flight track.

mineral dust is from a large dust storm which developed over the Gobi desert ~4 days prior to reaching the C130 flight track over the Yellow Sea. The measured average aerosol mass, based on the measured number distribution, and assuming a particle density of $2 \, g/cm^3$, was between 1900 and $2100 \, \mu g/m^3$, and the average surface area ranged from 1100 to $1250 \, \mu m^2/cm^3$ during this time leg.

Five-day backward trajectories for the air masses are shown in Fig. 1. The trajectories suggest that these masses first experience a strong injection of dust particles over the Gobi desert, which were then transported into Beijing and other populated Chinese urban centers in this region (such as Tianjin and Qingdao) at an altitude of ~500 m above sea level (asl). The air masses then travel off the continent and

passed through the MBL of the Yellow Sea until intercepted by the C130 on Flight #6. During the boundary layer advection over the ocean, the air masses are also likely exposed to injections of sea-salt particles.

3.1.2. Correlation analysis

ACE-ASIA C130 Flight #6 aerosol data contain a complicated set of cationic and anionic compounds. Of particular interest are the mineral compounds (i.e., Ca^{2+}, Mg^{2+}, and Na^+) since they alter the general equilibria of volatile and semi-volatile species. In order to see the probable cation–anion associations among the measured ionic compounds, a correlation and molar ratio analyses are carried out between the cations NH_4^+, Ca^{2+}, K^+, and Na^+, and the anions SO_4^{2-}, NO_3^-, and Cl^-. The results are shown in Fig. 2. In addition, Fig. 3
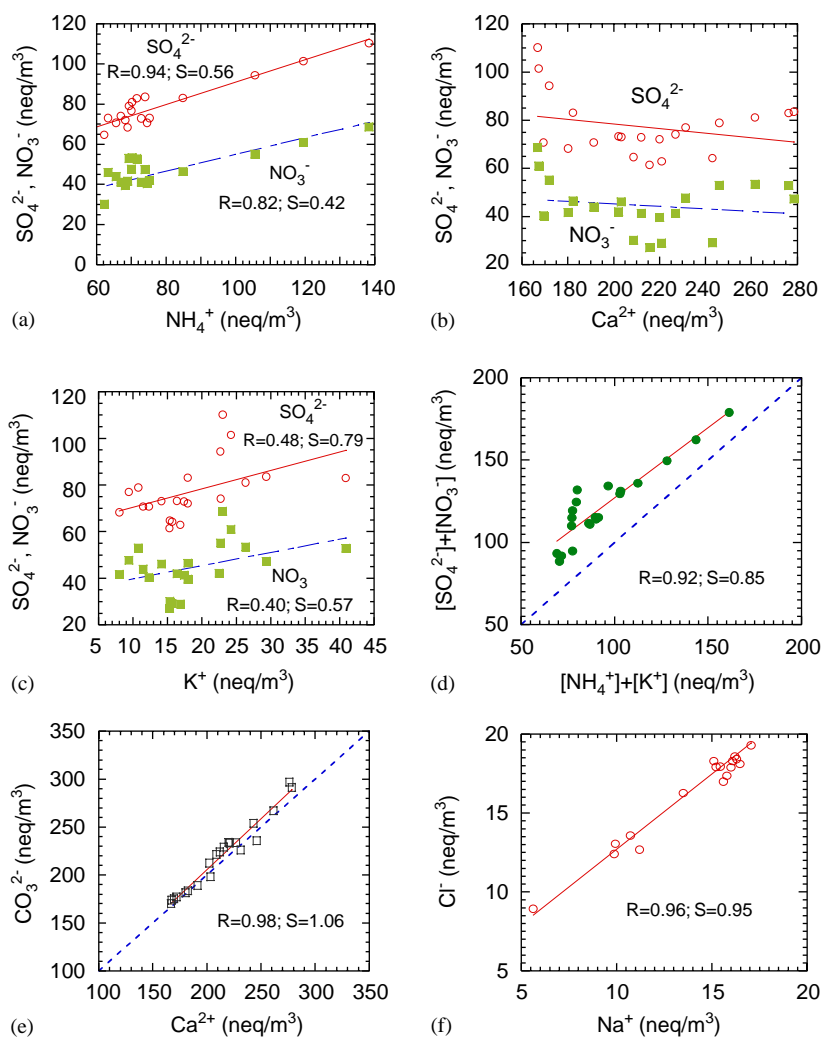

Fig. 2. (a)–(f) Correlation analyses between fine particle cations and anions for measurements in an air mass containing urban/industrial and mineral dust measured during ACE-Asia flight #6. In each panel, *R* and *S* represent the correlation coefficient and the slope of the linear plots, respectively.
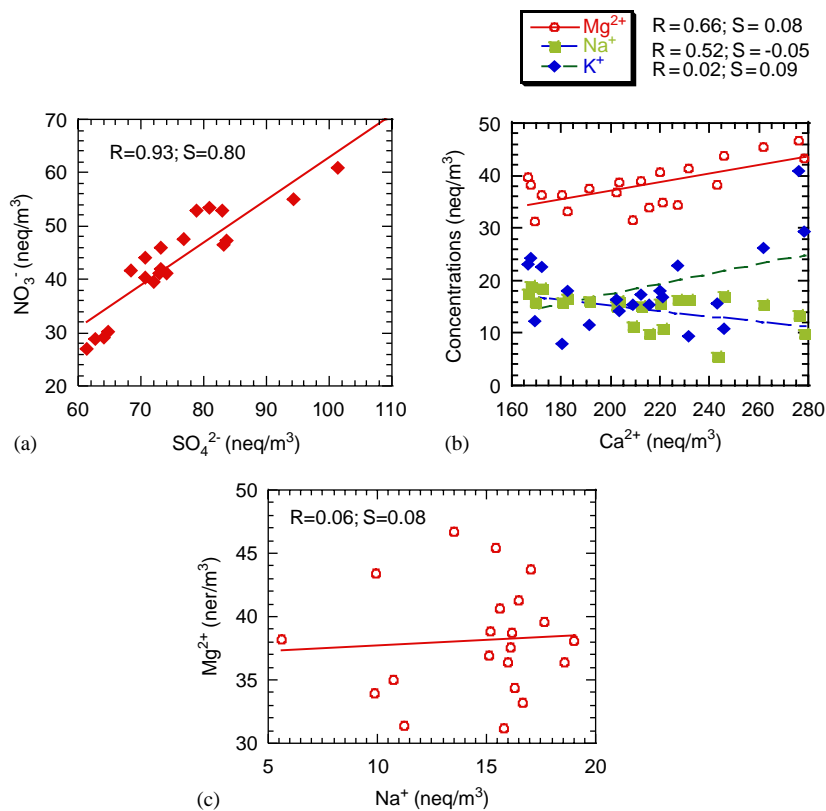
Fig. 3. (a)–(c) Correlations between the same charged ions for ACE-Asia Flight #6 to investigate co-located sources. In the each panels, R and S represent the correlation coefficient and the slope of the linear plots, respectively.

shows the correlations between the same charged ions. The purpose of the latter analysis is to investigate if the ion species are emitted from co-located sources. In this case, an overall ion balance is not undertaken since there is a large cation excess, apparently due to the presence of $CaCO_3$ and the lack of a CO_3^{2-} measurement (Lee et al., 2004; Maxwell-Meier et al., 2004). It is widely recognized that $CaCO_3$ (calcite) is a major compound in Asian mineral dust particles (Song and Carmichael, 1999, 2001b and references therein).

The correlations suggest that SO_4^{2-} is strongly associated with NH_4^+ (Fig. 2a: $R = 0.94$; $S = 0.56$) and moderately with K^+ (Fig. 2c: $R = 0.48$; $S = 0.79$), but not with Ca^{2+} (Fig. 2b). This implies that $2(NH_4^+)$–SO_4^{2-} could be a major cation–anion association, and that $2K^+$–SO_4^{2-} a minor association in the aerosol mixture. On the other hand, NO_3^- appears to be associated with NH_4^+ (Fig. 2a: $R = 0.82$; $S = 0.42$) and K^+ (Fig. 2c: $R = 0.40$; $S = 0.57$), but again not with Ca^{2+} (Fig. 2b). This could suggest some amount of NH_4^+–NO_3^- and K^+–NO_3^- in the aerosol mixture. However, Fig. 2b suggests that Ca^{2+} is not highly associated with SO_4^{2-} and NO_3^-. These findings are further confirmed in Figs. 2d and e. Fig. 2d shows a plot between

$[NH_4^+] + [K^+]$ and $[SO_4^{2-}] + [NO_3^-]$. Strong correlation ($R = 0.92$) and near unity molar ratio ($S = 0.85$) suggest that these cations are likely associated with these anions and are from urban sources. However, Ca^{2+} is almost perfectly associated with the estimated CO_3^{2-} concentration (Fig. 2e, $R = 0.98$; $S = 1.06$; again, note this 1-1 molar ratio). Carbonate is estimated by assuming that the particles are charge-neutral and that CO_3^{2-} is the only unmeasured anionic species. It follows then that the CO_3^{2-} concentrations ($[CO_3^{2-}]_{estimated}$) can be estimated by subtraction of the total measured anion equivalence from total measured cation equivalence, i.e.,

$$[CO_3^{2-}]_{estimated} = \sum_i^n [Cation]_{measured,i} - \sum_j^m [Anion]_{measured,j}, \qquad (1)$$

where n and m denote the total number of cations and anions measured by the PILS-IC instrument. It is widely recognized that $CaCO_3$ (calcite) is a major compound in the Asian dust particles (Song and Carmichael, 2001a,b and references therein), and it appears in this data that much of the fine particle $CaCO_3$ remains intact; the CO_3^{2-} not yet being replaced by NO_3^- and SO_4^{2-}.

Sea-salt particles are likely injected last into the air masses prior to detection as the air masses advected from the Asian continent to over the Yellow Sea where they were sampled. It is thus reasonable to expect that sea-salt particles would exist externally with the other particles because of the short amount of time for interaction both with other particles (i.e., coagulation) and acidic gases (i.e., condensation). Fig. 2f indicates a nearly perfect ion balance between Na^+ and Cl^- ($R = 0.96$; $S = 0.95$), reflecting the influence of sea-salt particles. Note that the mole ratio of Cl^- to Na^+ in sea-salt particles is 1.16, close to our value ($S = 0.95$) (Keene et al., 1986; Seinfeld and Pandis, 1998).

Based on these data, two observations are made: (1) both NH_4^+ and K^+ are likely associated with SO_4^{2-} and NO_3^- in a particle mixture; and (2) calcite ($CaCO_3$) remains almost intact in the dust particles.

A correlation analysis between the same charged ions suggests that NO_3^- and SO_4^{2-} are likely emitted from co-located sources (Fig. 3a: $R = 0.93$) and that Mg^{2+} and Ca^{2+} also originated from the same source (Fig. 3b: $R = 0.66$; $S = 0.08$), likely mineral dust from the Gobi desert. However, Ca^{2+} is not correlated with Na^+ and K^+ (Fig. 3b). As discussed previously, in this case the Na^+ originates mainly from seawater. K^+ seems to be emitted from local biomass (or bio-fuel) burning, being associated with both NO_3^- and SO_4^{2-} (Ma et al., 2003). Since sea-salt particles generally contain a large fraction of Mg^{2+} ($Mg^{2+}/Na^+ = 0.25$ on a mass basis) (Keene et al., 1986; Seinfeld and Pandis, 1998), Mg^{2+} and Na^+ is plotted in Fig. 3c. The pair is poorly correlated indicating that in this case they originated from different sources.

Time series plots along the measurement leg are shown in Fig. 4a and b. In Fig. 4a, the ionic correlations of $([Ca^{2+}] + [Mg^{2+}])_{measured}$ and $[CO_3^{2-}]_{estimated}$ are plotted. The mineral cations and carbonates are well correlated. Furthermore, the differences in the equivalence between the mineral cations and carbonates are small (note, the concentration scales are not to zero and thus the differences are amplified). Thus the majority of the dust particles throughout this airborne measurement leg are apparently un-reacted (i.e., dust particles still contain large amounts of $CaCO_3$). Fig. 4b presents the variations in the equivalences of cations $NH_4^+ – K^+$ and anions $SO_4^{2-} – NO_3^-$ along the airborne measurement leg.
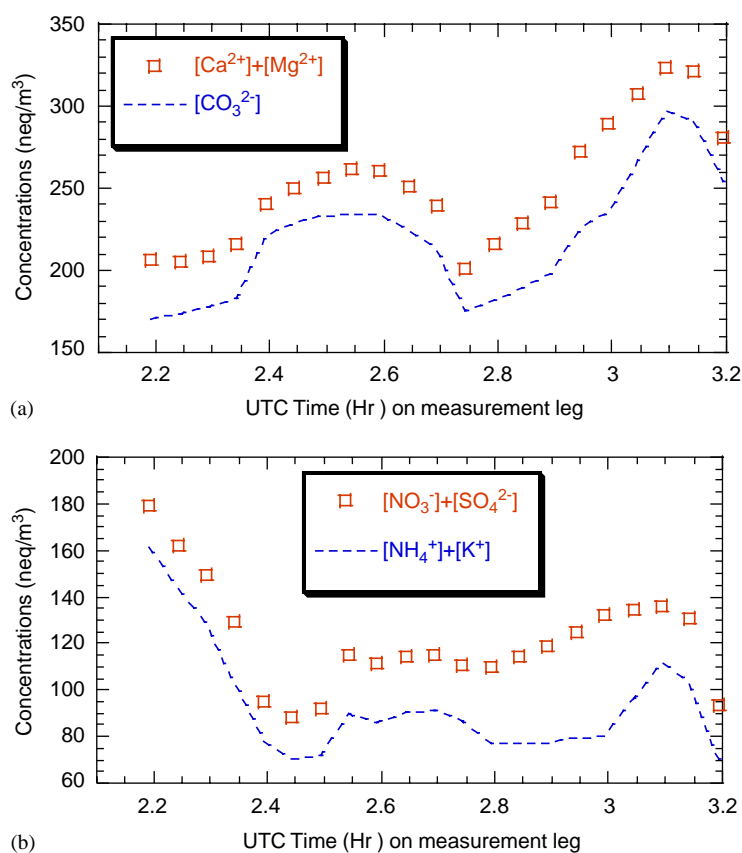

Fig. 4. Variations of measured cation and anion concentrations (neq/m^3) along the measurement leg of ACE-Asia C130 Flight#6: (a) $[Ca^{2+}] + [Mg^{2+}]$ and $[CO_3^{2-}]$; and (b) $[SO_4^{2-}] + [NO_3^-]$ and $[NH_4^+] + [K^+]$.

As shown in the scatter plots of Fig. 2, the cations and anions are well correlated throughout the whole measurement leg, and the excessive amounts in anion equivalence ($SO_4^{2-} + NO_3^-$) could be present in the dust particles. (Note that the differences between the two curves in Fig. 4a and b are similar due to the method for calculating carbonate, however, Fig. 4a does indicate that the inferred carbonate is lower and spatially well correlated with the mineral dust cations.)

The obvious defect of this analysis (Eq. (1)) is not to consider H^+ and OH^- equivalences. This is likely the largest uncertainty in determining carbonate concentrations by Eq. (1). However, as shown by Figs. 2e and 4, the estimated missing species (conjectured to be CO_3^{2-}) concentrations (possibly including the influences from H^+ and OH^- concentrations) tend to be nearly correlated 1-1 with the measured crustal Ca^{2+} concentrations. The temporal and spatial correlation between the estimated species (CO_3^{2-}) and the crustal Ca^{2+} strongly indicates that they have a similar source. Moreover, the near 1-1 equivalence ratios suggest the estimated species (CO_3^{2-}) is bound with crustal Ca^{2+}. Therefore, it seems reasonable to assume that the major unmeasured constituent during the C130 Flight #6 is CO_3^{2-}.

To estimate the fraction of carbonate replacement (FCR) in the dust particles the following formulas are used:

$$FCR(\%) = \frac{[CO_3^{2-}]_{replaced}}{[CO_3^{2-}]_{original}} \times 100, \quad (2)$$

$$[CO_3^{2-}]_{original} = [Ca^{2+}] + [Mg^{2+}], \quad (3)$$

$$[CO_3^{2-}]_{replaced} = [CO_3^{2-}]_{original} - [CO_3^{2-}]_{estimated}. \quad (4)$$

Here, the original CO_3^{2-} concentrations ($[CO_3^{2-}]_{original}$) are estimated from the equivalence concentrations of the two major mineral dust constituents $[Ca^{2+}] + [Mg^{2+}]$ (Eq. (3)). The replaced CO_3^{2-} concentrations ($[CO_3^{2-}]_{replaced}$) are estimated by the subtraction of the estimated CO_3^{2-} concentrations ($[CO_3^{2-}]_{estimated}$) from the original CO_3^{2-} concentrations ($[CO_3^{2-}]_{original}$). Again, the $[CO_3^{2-}]_{estimated}$ is calculated from Eq. (1). Using Eq. (2), the estimated FCR is in the range of 7–18% along the airborne measurement leg. Thus, by this method, the dust particles are estimated to contain only 7–18% sulfate and/or nitrate of the total anion equivalences.

It is noted that one mechanism by which two particles become internally mixed is coagulation. However, in our situation in which the focus is on only fine particles, coagulation is expected to be a slow process because the coagulation coefficients amongst the similar sized particles are very small (Wexler et al., 1994; also refer to Table 12.3 in p. 612 of Seinfeld and Pandis, 1998).

Collectively, the analyses suggest that the plume intercepted by the C130 during this period of Flight #6 contains mainly three different types of aerosols: mineral dust particles, anthropogenic urban particles (including biomass burning emissions), and sea-salt particles. If these plumes had only undergone limited interactions, component-wise, the aerosols are expected to be mainly composed of $2(NH_4^+)–SO_4^{2-}$, $NH_4^+–NO_3^-$, $Ca^{2+}–CO_3^{2-}$, and $Na^+–Cl^-$, with minor concentrations of $2K^+–SO_4^{2-}$ and $K^+–NO_3^-$ (note, the amount of K^+ is relatively small compared to the other cations). In order to further explore this finding, a "closed-mode" aerosol thermodynamic model is applied to these observations. In this case the focus is on the presence of $(NH_4)_2SO_4$ versus $CaSO_4$. The "closed-mode (or intra-particulate mode)" aerosol thermodynamic model is a technique to study the composition of the bulk aerosol, based on thermodynamic knowledge (Jacobson et al., 1996; Meng et al., 1998). Through the intra-particulate thermodynamic simulation, thermodynamically favorable intra-particulate ion associations among cations and anions are identified. Since only bulk ionic particle concentrations were measured by the PILS-IC during this study, the model simulations will be used to investigate the possible salts and ion associations for the dust and polluted urban aerosols recorded during the Yellow Sea measurements of Flight #6. The model will also be used to investigate the extent to which the dust particles are externally (or internally) mixed with the polluted urban particles.

3.1.3. Aerosol thermodynamic analysis

Thermodynamic intra-particulate aerosol simulations are performed (Jacobson et al., 1996; Meng et al., 1998), using the Simulating Composition of Aerosol Particles at Equilibrium II (SCAPE II) model. The SCAPE II model is one of many aerosol thermodynamic models available. The SCAPE II model is described in detail elsewhere (Kim and Seinfeld, 1993a,b; Meng et al., 1995), and thus only discussed briefly here. The aerosol thermodynamic model can predict the particle composition at the equilibrium state where the Gibbs free energy of the particulate phase is at a minimum. This implies that the intra-particulate conditions predicted by the thermodynamic model are in the most stable state for the given measured particle concentrations, RH, and temperature. It is widely accepted that the intra-particulate equilibria among various ions and salts are achieved so rapidly that one could theoretically examine the intra-particulate composition and/or associations with the aerosol thermodynamic model (Jacobson et al., 1996; Meng et al., 1998).

In order to simplify the simulation, it is first assumed that sea-salt particles ($Na^+–Cl^-$) exist externally to the other ionic components. This seems a reasonable assumption since the sea-salt particles were injected

last into the plume, and therefore they are least likely to have undergone interaction (e.g., coagulation) with other particles. This assumption is also consistent with the correlations. Secondly, Mg^{2+} is thought to be originated from soil rather than seawater, similar to Ca^{2+}. Thirdly, since the polluted urban aerosols and mineral dust particles have the longest contact times, only internal mixtures between these two types of aerosols are considered here.

In the simulation, the average aerosol composition, temperature, and RH over the time period of interest are used, however, actual values do not change drastically over the airborne measurement leg. Na^+ and Cl^- are removed from the internal mixture under the assumption that they exist as externally mixed sea-salt particles. Ca^{2+} and Mg^{2+} are added or subtracted into or out of the polluted urban aerosol particles assuming that the Mg^{2+} in the dust particles are lower than the Ca^{2+} by a factor of 0.1, on a mass basis. In order to define the degree of internal mixing (DIM_{Ca}) between the dust particles and the polluted urban aerosols, the following

formula is introduced:

$$\text{Degree of Internal Mixing (\%)} = \frac{[CaCO_3]_{int}}{[CaCO_3]_{tot}} \times 100,$$
(5)

where $[CaCO_3]_{tot}$ and $[CaCO_3]_{int}$ indicate the total measured mass of Ca^{2+} and the mass of Ca^{2+} that exists internally, respectively. The percentage of DIM_{Ca} defines how much the dust particles (represented by Ca^{2+}) are internally mixed with the polluted urban aerosols.

Fig. 5 shows how the anthropogenic urban aerosol composition could change with respect to DIM_{Ca}. Among the many ion combinations and salts shown in Fig. 5, particular attention should be paid to $2(NH_4^+)-SO_4^{2-}$ and $Ca^{2+}-SO_4^{2-}$, because our correlation analyses suggest that the former is a major combination in the fine polluted urban aerosol mixture, whereas the latter is unlikely formed. As DIM_{Ca} increases, the fraction of $2(NH_4^+)-SO_4^{2-}$ decreases, while the
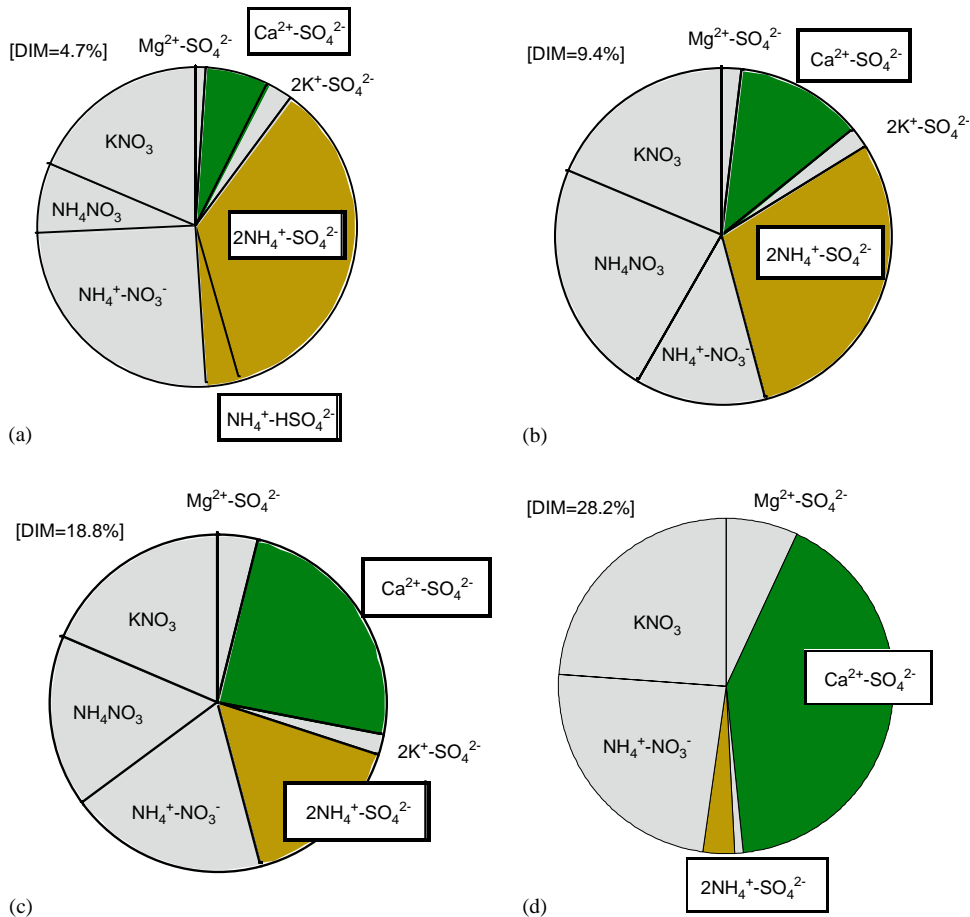

Fig. 5. (a)–(d) Composition changes of mixed mineral dust/urban particles predicted by SCAPE II as a function of the degree of internal mixing (DIM_{Ca}). The pie-charts are on a mole basis.

fraction of Ca^{2+}–SO_4^{2-} increases. At $DIM_{Ca} = 28\%$, $2(NH_4^+)$–SO_4^{2-} almost disappears and a large fraction of SO_4^{2-} is associated with Ca^{2+} and Mg^{2+}. Both the disappearance of $2(NH_4^+)$–SO_4^{2-} and the existence of Ca^{2+}–SO_4^{2-} are contradictory to our finding from the correlation analysis. Therefore, it appears that fine-mode dust particles (Ca^{2+} and Mg^{2+}) are mixed internally with the polluted urban aerosols (SO_4^{2-}) to an extent between 0% and ∼30% (i.e., they are mostly externally mixed). On the other hand, the fractions of the other ion-combinations (or salts) in the polluted urban particles, whose existences are conjectured through the correlation analysis (i.e., KNO_3, NH_4NO_3, NH_4^+–NO_3^-, and $2K^+$–SO_4^{2-}), do not vary greatly with DIM_{Ca}.

Also, it should be noted that since we use the intra-particulate mode of aerosol thermodynamic modeling in this study, in some cases the model predicts the presence of NH_2COONH_4 (s) (although it is not shown in Fig. 5), particularly at high DIM_{ca}. However, it appears that this is an artifact generated by using the "closed-mode" aerosol model. In the simulation, the added $CaCO_3$ and $MgCO_3$ alter the thermodynamic relations in the polluted urban particles. Particularly, at high DIM_{ca}, the relatively large amounts of carbonates from the added $CaCO_3$ and $MgCO_3$ make intra-particulate equilibria shift toward the formation of NH_2COONH_4 (s) with NH_4^+ that results from NH_4^-–SO_4^{2-} association (Meng et al., 1995) (as $CaCO_3$ is added into the polluted urban particles, NH_4^+ yields SO_4^{2-} to Ca^{2+}). However, the formation of NH_2COONH_4 (s) is very unlikely. If coalescence actually occurs between the polluted urban particles and $CaCO_3$, the carbonates would be dissipated from the particles instead of forming the NH_2COONH_4 (s). Thus, it appears that the formation of NH_2COONH_4 (s) is an unavoidable artifact when using the closed-mode aerosol model.

4. Other examples of inferred dust mixing state in the MBL of the Yellow Sea

The subsequent ACE-Asia C130 flight (Flight#7) was also flown into the MBL of the Yellow Sea (Maxwell-Meier et al., 2004). Back trajectory analyses for the air masses that arrived in the measurement leg again show that the air masses could be a mixture of dust and anthropogenic urban particles (although not shown). The analyses of particulate composition along two measurement legs of this flight are shown in Fig. 6. Following the same procedures as for Flight#6, the carbonate concentrations shown in Fig. 6 are estimated by Eq. (1). The first leg covers from 3:16 to 4:16 UTC April 12, 2001, and the second leg was measured between 5:43 to 6:31 UTC April 12, 2001. During the two legs, high Ca^{2+} and SO_4^{2-} concentrations were also

measured in the MBL of the Yellow sea along almost the same measurement track as ACE-ASIA C130 Fligt#6 (a North-South flight track on 124.22°E longitude between 33–37°N latitude). Application of the same methodology to this flight leads to the same conclusions; that there is a large degree of external mixing between fine dust and the fine polluted urban particles. As shown in Fig. 6, mineral dust particles along the airborne measurement track still contain large amounts of carbonates (i.e., mostly composed of $CaCO_3$), whereas the polluted urban particles are mainly composed of NH_4^+–K^+–SO_4^{2-}–NO_3^-.

5. Uncertainties associated with water uptake by the aerosol particles

The mixed dust/pollution/sea-salt plumes of the C130 Flight #6 have relatively high RHs of ∼59%. Furthermore, the salts formed in the dust/pollution/sea-salt plumes case, shown in Fig. 5, would have low deliquescent relative humidities (DRHs). Thus, the particles will take up some amount of water, and cation and anion electrolytes would dissolve in the aqueous phase. When this occurs, one could question how the ion-pairs are assigned among the electrolytes in the aqueous phase.

In our approach, we first postulate that the ions in the aqueous phase are associated with each other, even if they exist separately in the aqueous phase. Theoretically, the total ion balance in the aqueous phase should be met. In this process, each cation is preferentially neutralized by a specific anion or anions (or vice versa). Based on this assumption, the pairing between cations and anions is conducted, considering thermodynamic preferences. For example, when RH (or the amount of particulate water) is gradually decreased in a Ca^{2+}–K^+–NH_4^+–SO_4^{2-} system, $CaSO_4$ precipitate first, followed by K_2SO_4. The reduction of particulate water makes both binary activity coefficients (γ's) and molarity of ion species increase, and thus the salt–ion equilibria are shifted towards the salt formation (i.e., precipitation). We have assumed that every ion in the aqueous phase is in equilibrium with the salts, even when the salt concentrations are zero (i.e., no precipitation). A salt–ion equilibrium between NH_4NO_3 and NH_4^+–NO_3^- can be conjectured in Fig. 5, because of their co-existence. When the salt concentration is 0 (e.g., $2NH_4^+$-SO_4^{2-} and $(NH_4)_2SO_4$ in Fig. 5), the salt–ion equilibrium is assumed to be shifted toward complete ion formation. In this case, the salts being in equilibrium with aqueous-phase ions can be visualized by a gradual decrease in RH. We have used this simulated precipitation method to investigate the thermodynamic preferences (or affinity) by which the cations and anions are neutralized in the aqueous phase and the ion
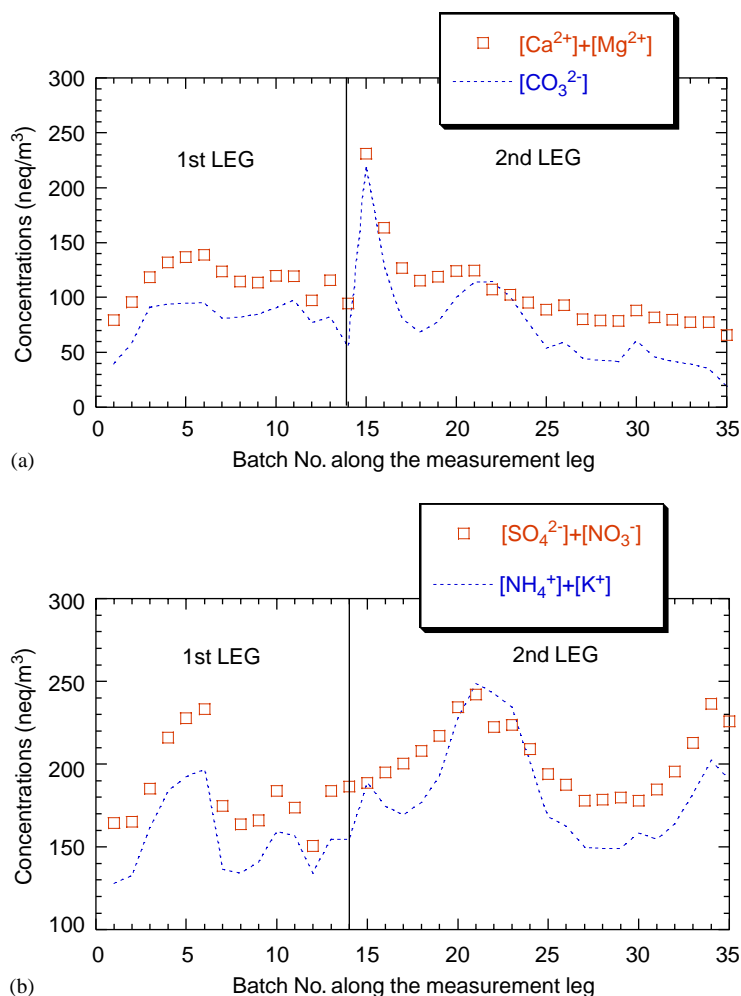
Fig. 6. Variations of measured cation and anion concentrations (neq/m^3) along the airborne measurement legs of ACE-Asia C130 Flight#7: (a) $[Ca^{2+}]+[Mg^{2+}]$ vs. $[CO_3^{2-}]$ for mineral dust particles; and (b) $[SO_4^{2-}]+[NO_3^-]$ vs. $[NH_4^+]+[K^+]$ for polluted urban particles.

associations shown in Fig. 5 are made by the method explained above.

6. Conclusions

Three and one-half minute integrated aerosol inorganic composition data from measurements during ACE-ASIA C130 Flight #6 are analyzed to investigate the fine-mode particle mixing state. In this case study, dust-laden air masses are mixed with urban air pollutants over Beijing and Tianjin areas. The dust aerosol plumes mixed with the polluted urban aerosols were recorded in the MBL of the Yellow Sea. The analysis focuses on the mineral dust/urban pollution interactions. Backward trajectories indicate these two air masses were mixed ~1.2 days prior to the measurements. Correlations between various fine-particle ionic

compounds suggest the existence of $2NH_4^+$–SO_4^{2-} in the aerosol mixture, but the measured Ca^{2+}–SO_4^{2-} ions are apparently not highly associated. The thermodynamic aerosol simulations, assuming various degrees of external (or internal) mixing, indicate that the $2NH_4^+$–SO_4^{2-} associations are only possible when dust particles (Ca^{2+}) and polluted urban aerosol (SO_4^{2-}) are externally mixed to a large degree. In this case the degree of internal mixing (by Ca^{2+} mass) is estimated to range between approximately 0% and 30%, or the degree of external mixing by Ca^{2+} mass is larger than 70%).

A similar finding is also reported by Zhang et al. (2003), who analyzed individual particles using electron microscopes and an energy dispersive X-ray (EDX) spectrometer. This study was also conducted during periods of ACE-ASIA (March–May, 2001) at Qingdao, a site located near to the airborne measurement leg of ACE-ASIA C130 Flight#6 (the city is located at the

seashore of the Yellow Sea, 120.2°E and 36.05°N; refer to Fig. 1). Thus, they are also likely analyzing plumes in which pollution had recently mixed with mineral dust. They report that ~90% of the dust particles were fresh dust that did not contain sulfate or nitrate. Thus, the dust particles were almost pure, not being greatly affected by, or interacting with, anthropogenic pollutants. Through the use of model simulations, we are currently investigating why acidic gases produced in the urban plume did not substantially interacted with the mineral dust particles during the roughly 30 h between mixing over the urban regions and detection in the Yellow Sea boundary layer (e.g., ACE-ASIA C130 Flight#6). This study is aimed at understanding the chemical processing of dust and reactive acidic pollutants by focusing on specific plumes. The observation of limited reaction between fine particle dust and pollutants observed in this case cannot be generalized to the region. Other measurements of possibly more aged dust show evidence for significant dust-pollution interaction (Wu and Okada, 1994; Choi et al., 2001).

References

Choi, J.C., Lee, M., Chun, Y., Kim, J., Oh, S., 2001. Chemical composition and source signature of spring aerosol in Seoul, Korea. Journal of Geophysical Research 106, 18,067–18,074.

Cooke, W.F., Wilson, J.J.N., 1996. A global black carbon aerosol model. Journal of Geophysical Research 101, 19395–19409.

Covert, D.S., Heintzenberg, J., 1984. Measurement of the degree of internal/external mixing of hygroscopic compounds and soot in atmospheric aerosol. The Science of the Total Environment 36, 347–352.

Haywood, J.M., Roberts, D.L., Slingo, A., Edwards, J.M., Shine, K.P., 1997. General circulation model calculations of the direct radiative forcing by anthropogenic sulfate and fossil-fuel soot aerosol. Journal of Climate 10, 1562–1577.

Jacobson, M.Z., Tabazadeh, A., Turco, R.P., 1996. Simulating equilibrium with aerosols and non-equilibrium between gases and aerosols. Journal of Geophysical Research 101, 9079–9091.

Keene, W.C., Pszenny, A.A.P., Galloway, J.N., Hawley, M.E., 1986. Sea-salt correlations and interpretation of constituent ratios in marine precipitation. Journal of Geophysical Research 91, 6647–6658.

Kim, Y.P., Seinfeld, J.H., 1993a. Atmospheric gas–aerosol equilibrium I. Thermodynamic model. Aerosol Science and Technology 19, 157–181.

Kim, Y.P., Seinfeld, J.H., 1993b. Atmospheric gas–aerosol equilibrium II. Thermodynamic model. Aerosol Science and Technology 19, 182–198.

Kleeman, M.J., Cass, G.R., Eldering, A., 1997. Modeling the airborne particle complex as a source-oriented external mixture. Journal of Geophysical Research 102, 21355–21372.

Lee, Y.-N., Weber, R.J., Ma, Y., Orsini, D., Maxwell, K., Blake, D., Meinardi, S., Sachse, G., Harward, C., Clarke, A.D., Moore, K., Kapustin, V.N., Chen, T.-Y., Thornton, D.C., Tu, F.H., Bandy, A.R., 2003. Airborne measurement of inorganic ionic components of fine aerosol particles using the PILS-IC technique during ACE-ASIA and TRACE-P. Journal of Geophysical Research 108 (D23), 8046.

Ma, Y., Rodney, R.J., Lee, Y.-N., Thornton, D.C., Bandy, A.R., Clarke, A.D., Blake, D.R., Sachse, G.W., Fuelberg, H.E., Kiley, C.M., Woo, J.-H., Streets, D.G., Carmichael, G.R., Eisele, F.L., 2003. The characteristics and influence of biosmoke on fine particle ionic composition measured in Asian outflow during TRACE-P. Journal of Geophysical Research 108, 8816 NOV. 4.

Maxwell-Meier, K., Weber, R.J., Song, C.H., Orsini, D., Ma, Y., Carmichael, G.R., Streets, D., Blomquist, B., 2004. Inorganic composition of particles in mixed mineral dust-pollution plumes observed from ACE-ASIA. Journal of Geophysical Research 109, D19507.

Meng, Z., Seinfeld, J.H., Saxena, P., Kim, Y.P., 1995. Atmospheric gas–aerosol equilibrium: IV. Thermodynamics of carbonates. Aerosol Science and Technology 23, 131–154.

Meng, Z., Dabdub, D., Seinfeld, J.H., 1998. Size-resolved and chemically resolved model of atmospheric aerosol dynamics. Journal of Geophysical Research 103, 3419–3435.

Orsini, D., Ma, Y., Sullivan, A., Sierau, B., Baumann, K., Weber, R., 2003. Refinements to the Particle-Into-Liquid Sampler (PILS) for ground and airborne measurements of water soluble aerosol composition. Atmospheric Environment 37, 1243–1259.

Seinfeld, J.H., Pandis, S.N., 1998. Atmospheric Chemistry and Physics: Air Pollution to Climate Change. Wiley, New York.

Song, C.H., Carmichael, G.R., 1999. The aging process of naturally emitted aerosol (sea-salt and mineral aerosol) during long range transport. Atmospheric Environment 33, 2203–2218.

Song, C.H., Carmichael, G.R., 2001a. Gas–particle partitioning of nitric acid modulated by alkaline aerosol. Journal of Atmospheric Chemistry 40, 1–22.

Song, C.H., Carmichael, G.R., 2001b. A three-dimensional modeling investigation of the evolution processes of dust and sea-salt particles in East Asia. Journal of Geophysical Research 106, 18131–18154.

Weber, R.J., Orsini, D., Daun, Y., Lee, Y.-N., Klotz, P., Brechtel, F., 2001. A particle-into-liquid collector for rapid measurements of aerosol chemical composition. Aerosol Science and Technology 35, 718–727.

Wexler, A.S., Lurmann, F.W., Seinfeld, J.H., 1994. Modeling urban and regional aerosols—I. Model development. Atmospheric Environment 28, 531–546.

Wu, P.M., Okada, K., 1994. Nature of coarse nitrate particles in the atmosphere—a single particle approach. Atmospheric Environment 28, 2053–2060.

Zhang, X.Q., McMurry, P.H., Hering, S.V., Casuccio, G.S., 1993. Mixing characteristics and water content of submicron aerosols measured in Los Angeles and at the Grand Canyon. Atmospheric Environment 27A, 1593–1607.

Zhang, D., Zhang, J., Shi, G., Iwasaka, Y., Matsuki, A., Trochkine, D., 2003. Mixture state of individual Asian dust particles at a coastal site of Qingdao, China. Atmospheric Environment 37, 3895–3901.